Analysis of the effect of shoring in the behaviour of reinforced concrete slabs

David Simavorian

Master Thesis in Civil Engineering

Extended abstract

Supervisors

Professor Doctor Luís Manuel Soares dos Santos Castro

Professor Doctor Jorge Manuel Caliço Lopes de Brito

Jury

President: Professor Doctor Luís Manuel Coelho Guerreiro

Supervisor: Professor Doctor Jorge Manuel Caliço Lopes de Brito

Members: Professor Doctor João António Teixeira de Freitas

May 2015

1. Introduction

The design of reinforced concrete slabs in current building structures generally concerns the structure in its final shape and only considers the actions and the strength of concrete at 28 days. Thus the entire history of stress and strain distributions installed in the slab before 28 days is not considered. However, most of the collapses of reinforced concrete structures are due to problems related to the construction stage, in particular the definition of the slab shoring system.

Therefore, since the constructive process has a great impact on the proper implementation of reinforced concrete structures it is essential to design conveniently all the shoring system in particular the spacing between the shores, the date and the sequence of withdrawal of the shores.

The purpose of this work is to study the influence that the construction stage has on the distribution of stresses and strains installed in slabs before and after the complete removal of the shoring system. To that purpose, a numerical model for the analysis of concrete's thermo-mechanical properties evolution over time has been developed. This model was then used to simulate the behaviour of several alternative procedures to define the shoring system that can be adopted in the construction phase with the aim of identifying the best practices to reduce the probability of concrete cracking before total withdrawal of the shores.

2. Numerical simulation: Thermal and mechanical analysis

In order to analyse the effect of the shoring on the distribution of stress and strains installed in slabs it was necessary to model the behaviour and the evolution of mechanical and thermal properties of the concrete. This modelling was performed with the aid of the finite element commercial code ADINA (Automatic Dynamic Incremental Nonlinear Analysis).

The Adina (2011) program has the ability to solve a wide variety of mechanical and thermal problems. The program provides capabilities for the stress analysis of solids (2D and 3D) and structures considering static and dynamic loadings. It also allows the implementation of linear or nonlinear analyses and has a large amount of constitutive concrete models that allows the implementation of analysis that takes into account the temperature, creep and crack, among others. In addition to the existing materials in the program, the ADINA enables the creation of new constitutive relations that can be included in the program.

Thus, based on the Adina program the analysis process started with the analysis of heat (temperature) distribution caused by the internal heat generation (due to cement hydration) and the heat transfer process between the concrete slab and the environment, and then the result of the heat analysis was used to carry out an analysis of the stress and strain distributions installed in the structure.

2.1. Thermal analysis

All the phenomena involved in the thermal analysis of concrete can be seen in Figure 1. It should be noted that the solar radiation was not considered in the analysis carried out in this work since the slab under study is re-

lated to a structural floor. However, it is important to note that when the thermal analysis is performed on roof slabs the solar radiation effects are very relevant because they can significantly increase the temperature and thermal stress on the slab.

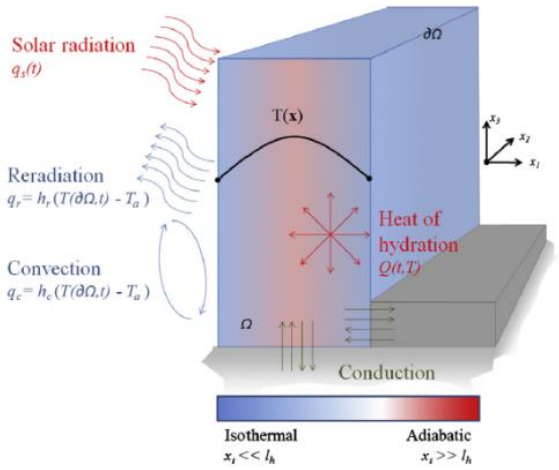

Figure 1 - Schematic representation of the phenomena involved in the chemo-thermal analysis of concrete (Honorio *et al.*, 2014)

The determination of the value of the temperature field of the concrete, taking into account the internal heat generation and the boundary conditions is based on the Fourier law (equation 1),

$$\frac{\partial}{\partial x}\left(k\,\frac{\partial T}{\partial x}\right) + \frac{\partial}{\partial y}\left(k\frac{\partial T}{\partial y}\right) + \frac{\partial}{\partial z}\left(k\frac{\partial T}{\partial z}\right) + \dot{Q} = \rho c\,\frac{\partial T}{\partial t} \tag{1}$$

where k is the thermal conductivity, ρc the heat capacity, T the temperature, t the time and $\dot{Q}$ the internal heat generation rate of the mix. The value of $\dot{Q}$ was determined based on the results obtained by Azenha (2009) for a cement CEM I 42.5R. Figure 2 illustrates the considered values in this work for the internal heat generation.

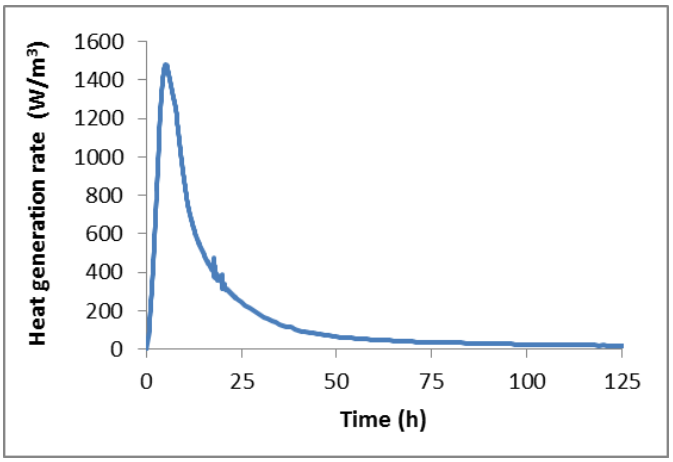

Figure 2 - Evaluation of heat generation rates over time

The boundary conditions (convection and radiation) are described by equations 2 and 3, respectively,

$$q_c = h_c(T_s - T_A) \tag{2}$$

$$q_r = \varepsilon\sigma(T_s^4 - T_A^4) \tag{3}$$

where q_c is the convective heat flux, $(T_s - T_A)$ the temperature difference between the concrete surface and the environment, h_c the convection heat transfer coefficient, q_r the radiative heat flux, ε the radiative property of the surface, referred to as *emissivity*, and σ the Stefan-Boltzmann constant.

Table 1 shows all the thermal properties of concrete considered in numerical modelling.

Table 1 - Concrete thermal properties

Thermal properties	
K (W.m^{-1}.K^{-1})	2.6
ρ (kg/m^3)	2360.7
c (J.kg^{-1}.K^{-1})	900
h_c (W.m^{-2}.K^{-1})	10
ε	0.88
σ (W.m^{-2}.K^{-4})	5.67E-08

2.2. Mechanical analysis

Based on the results obtained by the thermal model, the mechanical behaviour of concrete was modelled over time, in particular the evolution of the elastic modulus, the creep and the shrinkage. Since none of the constitutive models existing in ADINA allowed performing the desired analysis, a new constitutive model was added (based on totally new and already existing routines written in Fortran) and this model was used in the ADINA program to perform the parametric studies.

The evolution of the elastic modulus of the concrete was one of the main parameters considered in the numerical model. In fact, this parameter has a great relevance in the concrete modelling at early ages, especially before 28 days, since their value strongly influences the value of the stress and strains installed in concrete. The evolution of this parameter over time was determined based on the following equations:

$$E_{ci}(t) = \beta_E(t).E_{ci} \tag{4}$$

$$E_{ci} = \alpha_E \, E_{c0} \, (\frac{f_{cm}}{f_{cm0}})^{\frac{1}{3}} \tag{5}$$

$$\beta_E(t) = \sqrt{\beta cc(t)} \tag{6}$$

where E_{ci} is concrete's modulus of elasticity (MPa) at 28 days, $E_{ci}(t)$ concrete's modulus of elasticity (MPa) at age t, E_{c0} is equal to 21500 MPa, $\beta_E(t)$ a coefficient which depends on the age of the concrete *t,* α_E a coefficient which depends on the type of aggregates, f_{cm} the mean compressive strength at 28 days, f_{cm0} is equal to 10 MPa and t the equivalent age of the concrete in days.

Another parameter considered in the modelling of the behaviour of the concrete was creep. This parameter is quite relevant in the numerical analysis of concrete. According to De Shutter and Kovler (2001) the creep deformation of concrete at early ages can strongly influence the stress state of the structure because it causes a

decrease to about half of the volumetric and thermal stress. Concrete creep can also cause a significant increase in long-term deformations.

In this dissertation the formulation used to predict the evolution of concrete creep over time was the Double Power Law (DPL) (Bazant e Chern, 1985). Several studies show that the DPL formulation has a good coherence with experimental campaigns devoted to creep behaviour of concrete mainly at early ages. Figure 3 shows the comparison between the experimental results (developed by Azenha) and the results obtained by the DPL formulation. It is noted that, in fact, the DPL model has a very good coherence with the experimental values. Therefore, it is considered that the use of the DPL is reasonable for the applications in this dissertation, and it was adopted by considering the following creep compliance function at time *t*, for a load applied at instant *t'* (both times expressed in days):

$$J(t,t') = \frac{1}{E_0} + \frac{\phi_1}{E_0}.((t')^{-m} + \alpha_{DPL}).(t-t')^n \quad (7)$$

where E_0 is the asymptotic elastic modulus (corresponding to short term loads), and ϕ_1, m and n material parameters, calibrated based on experimental creep tests.

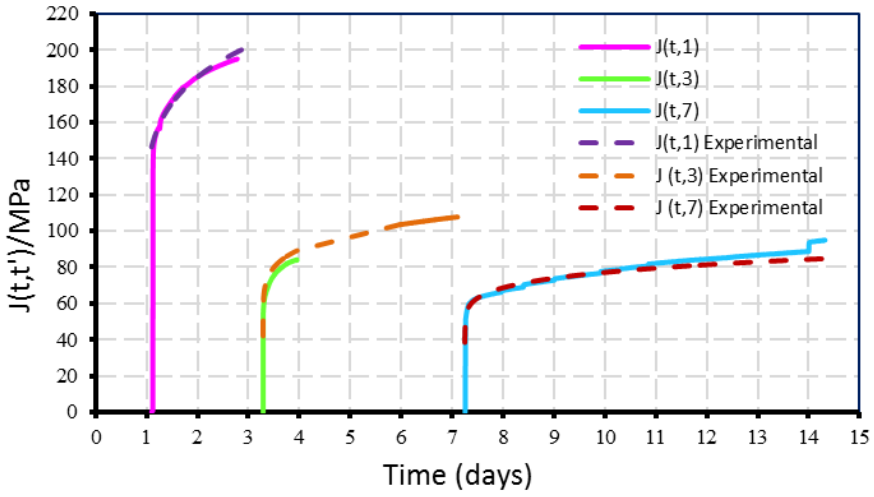

Figure 3 - Comparison of the values of creep obtained by experimental analysis and with double creep law expressions

Table 2 shows the values considered for the parameters present in equation 7.

Table 2 - Double creep law parameters

E_0 (GPa)	ϕ_1	m	n	α_{DPL}
23.8	2.15	0.48	0.19	0.05

Shrinkage is another relevant parameter in the numerical analysis of concrete structures. The modelling of the evolution of shrinkage over time was performed based on the equation listed in EN 1992-1-1 (2004). Thus the equivalent shrinkage temperature was determined and then applied to the slab under study. Figure 4 illustrates the evolution of the equivalent shrinkage temperature over time considered in the numerical simulation.

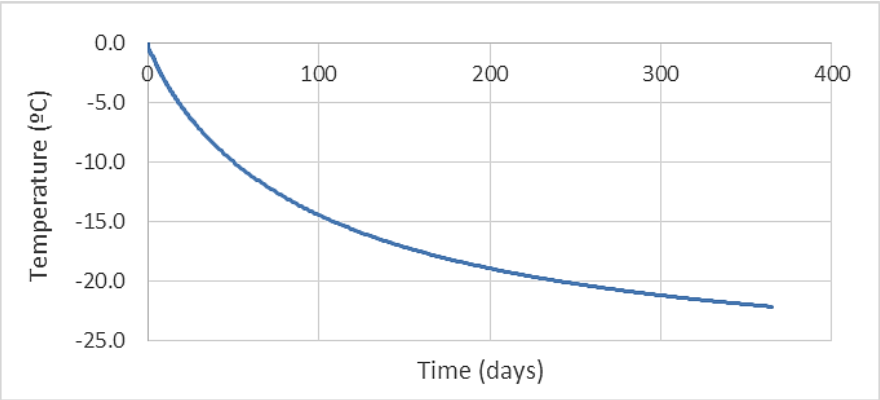

Figure 4 - Shrinkage equivalent temperature

3. Parametric study

Using the numerical model implemented, the repercussions of the stress and strain distributions installed in the slab during the constructive stage on the design of slabs and the verification of the serviceability limit states (SLS) during the lifetime of the structure were assessed.

At first, a model (designated as the base model) assuming a set of parameters in the shoring system usually found in current building projects was considered. Based on this model the impact of the temperature, the evolution of the modulus of elasticity of concrete and its rheological properties (creep and shrinkage) on the early ages of concrete was studied. The consequences of neglecting those effects on the long-term were also evaluated. Subsequently, several other studies were performed in which the conditions of the problem were modified, in particular the spacing of props, the geometry and the boundary conditions of the slab, the plan and date of withdrawal of props and the period of the year in which concrete casting of the slab occurs (summer/winter). Finally, the consequences of these changes on the distribution of stress and strains installed in the slab before and after the total shoring removal were characterised.

3.1. Model 1 (base model)

3.1.1. Model 1 description

The geometry of the model 1 (base model) comprises a 6 m square slab of reinforced concrete 0.20 m thick. The slab has edge beams 0.25 m wide and 0.50 m high and corner columns with a cross-section of 0.25 m x 0.25 m. The height of the columns is 3 m. The concrete used in this work belongs to class C25/30 and the cement is CEM I 42.5 R (with a content of 240 kg/m^3).

In order to support the actions that act on the structure at the early ages and its self-weight at a time when the concrete still does not have enough strength to be self-supporting, a shoring system formed by wooden planks (which support the slab), secondary and primary beams (used to support the wooden planks) and steel props (which support the entire weight of the shoring system and all the actions that act on the slab during the construction phase), was included in the numerical model.

In model 1, the secondary beams are spaced 0.6 m and the primary beams, as well as the props, have a spacing of 1.5 m. Table 3 shows the mechanical properties of steel and wood that constitute the shoring system and Table 4 illustrates the cross-sections considered for the shoring elements.

Table 3 - Mechanical properties of the shoring system elements

	Steel	Wood
Elastic modulus - E (GPa)	210	7
Poisson´s ratio - ν	0.3	0.3
Density - ρ (kg/m^3)	77	5
Coefficient of thermal expansion- α_T (ºC^{-1})	1.20E-05	3.00E-06

Table 4 - Shoring system elements dimensions

Shoring system elements	Dimensions
Wooden planks (thickness)	2.5 (cm)
Secondary beams	8 x 16 (cm^2)
Primary beams	8 x 16 (cm^2)
Props	D_{ext}: 50 (mm); e: 2.2 (mm)

Figure 4 illustrates the numerical model of the slab with the definition of the elements of the shoring.

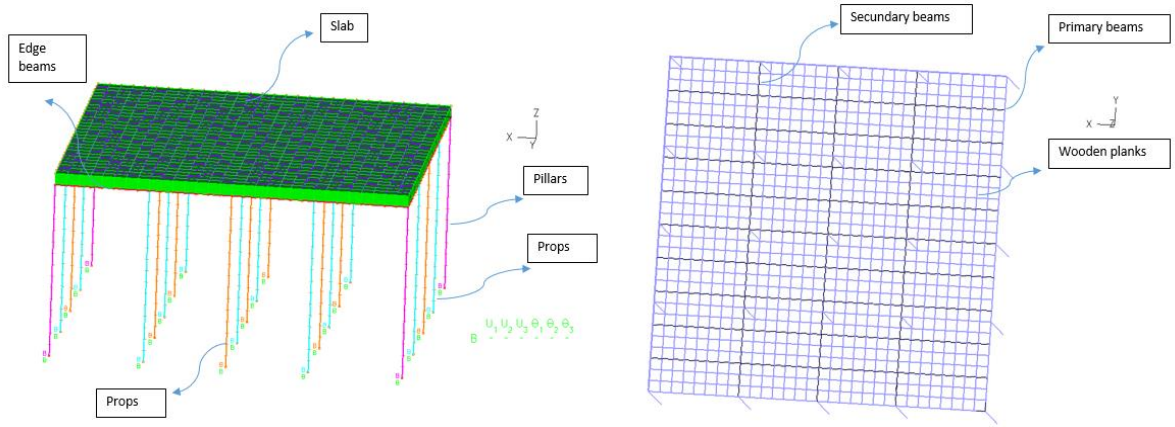

Figure 4 - Numerical model of the slab and shoring system

The period of numerical analysis in the base model was 1 year (beginning in June 1st). Since this period of time is very large, the numerical model of the ADINA was run considering time steps with increasing value:

- first 7 days: 1 h;
- from 7 days to 14 days: 2 h;
- from 14 days to 28 days: 4 h;
- from 28 days to 365 days: 24 h.

Regarding the actions acting on the structure, different values for the prescribed loads and the remaining permanent loads have been considered, according to the considered time period (Table 5).

Table 5 - Structure vertical load values

	Load values (kN/m^2)
Structure deadweight	5
Remaining permanent load (after 28 days)	1.5
Partition walls (after 28 days)	1.8
Prescribed load (between 3 and 28 days)	1.5
Prescribed load (after 28 days)	3

According to the actions described and the stress resultants that occur in the ultimate limit states (ULS), a reinforcement of #ϕ12//0.20 and #ϕ8//0.20 at the top and bottom of the slab, respectively, was considered. This reinforcement was explicitly considered in the numerical model.

The numerical analysis in this work was essentially performed in terms of serviceability limits state and not so much from a ultimate limit state perspective. Thus, the combinations of actions considered were the following:

- Quasi-permanent combination: to check the limit state of deformation and cracking;
- Characteristic (rare) combination: to verify the occurrence of localized cracking.

The removal of the shoring system was performed gradually during the time period considered in the numerical analysis. Up to 7th day all the shoring was maintained and after that period about 60% of existing props were removed. Finally, at 28 days, all the shoring system and formwork were removed. The shoring removal scheme over time is presented in Figure 5.

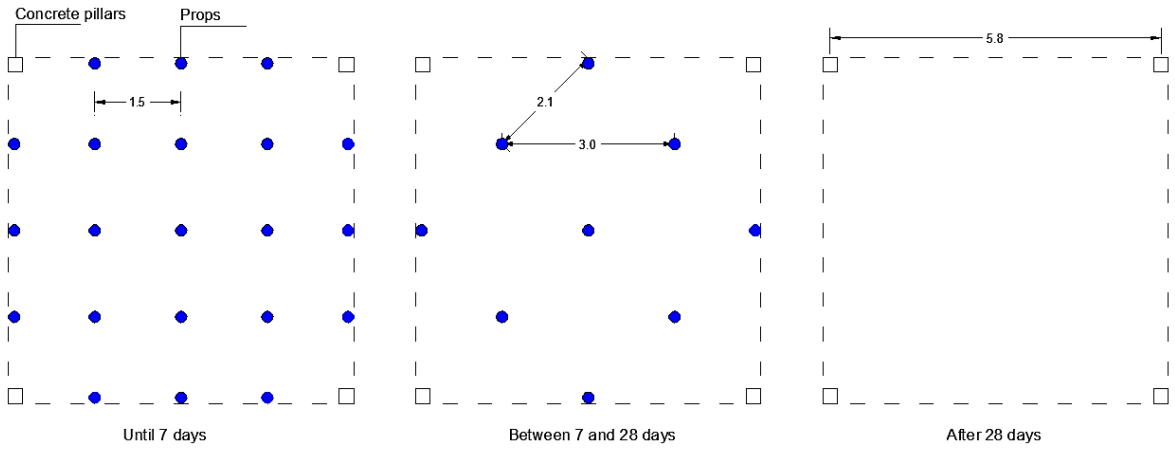

Figure 5 - Shoring removal scheme over time

3.1.2. Model 1 numerical analysis

Based on the described model a study was carried out on the impact that creep, temperature and shrinkage have on the values of the stress and deformation distributions, before and after the complete withdrawal of the props. Based on this study it was found that, in model 1, shrinkage cannot by itself cause slab cracking or contribute significantly to the value of the total stress. However, the same is not true about the thermal stress (resulting from temperature variations) that is significantly more relevant than shrinkage. This is illustrated in

Figure 6, which shows the evolution of tensile stress on the bottom of the slab mid-span over time for the characteristic combinations.

Analysing the results, it is possible to verify that the period of autumn/winter is when the greater tensile stresses occur in the slab. In fact, during the winter period maximum tensile stresses of approximately 0.8 MPa have been observed. However, even though the tensions due to temperature already had a significant value, temperature by itself does not cause any cracking of the structure since tensile stresses are still far below the axial tensile strength (f_{ctm}) and the flexural tensile strength, $f_{ctm,fl}$.

In what concerns creep, until the complete removal of the props, there is not a significant difference of deformations with and without considering that effect. In fact, until 27 days, the deformation without creep were 0.81 mm, only 0.1 mm less than the one with creep. However, after the complete withdrawal of the shoring system, there is a clear difference between the two models. In fact, after one year the deformation without creep is approximately 4.5 mm, about 1.9 times lower than the one with creep (Figure 7).

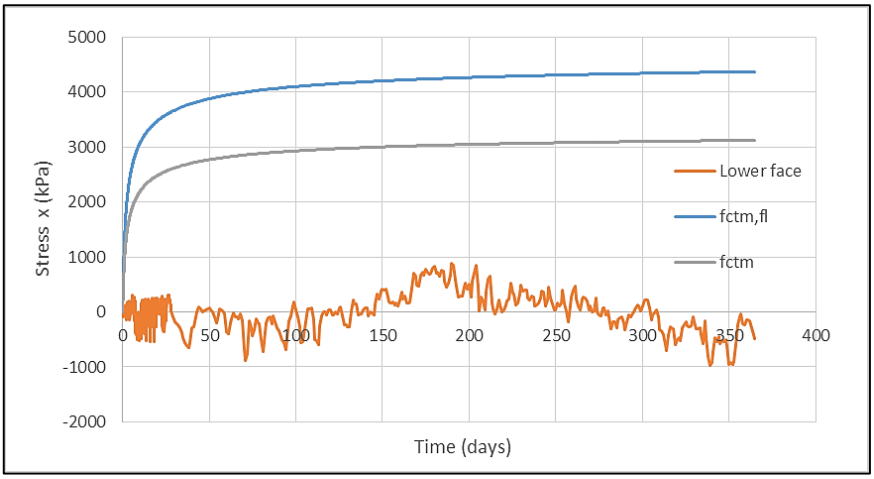

Figure 6 - Comparison of tensile stresses at mid-span of the slab due to temperature with the tensile strength of concrete

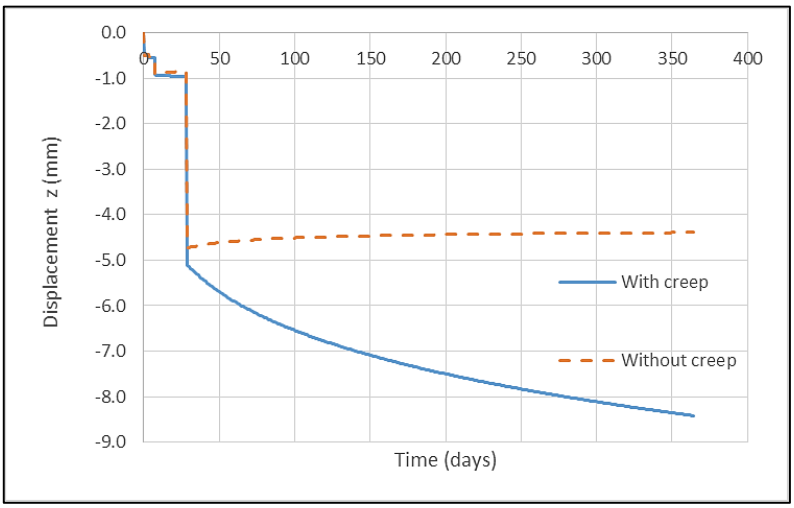

Figure 7 - Vertical deformation with and without creep in the slab mid-span

Figure 8 represents the stress components for the characteristic combination due to shrinkage, temperature and loading (with creep), as well as the value of total stress. It is obvious that the vertical loads have the great-

est impact on total stresses. However, it is temperature that causes an increase of tensile stresses (particularly in winter) and an increase of compressive stresses (particularly in summer).

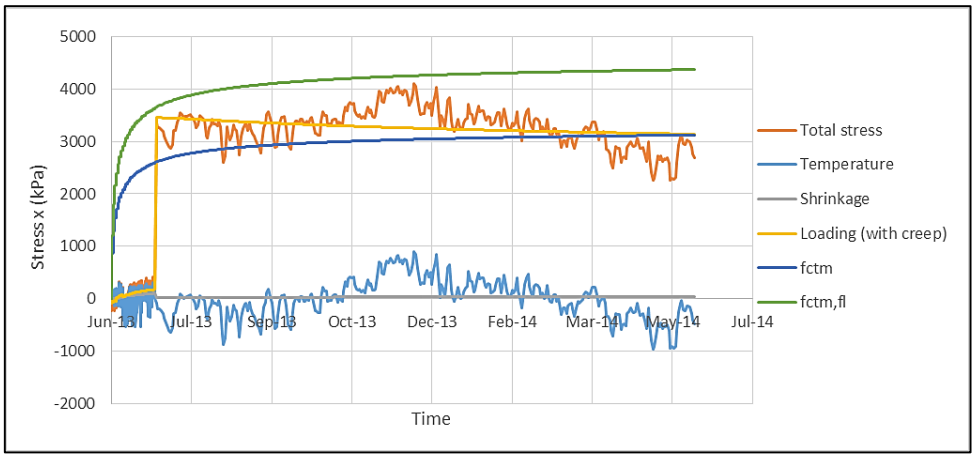

Figure 8 - Variation of the total and partial stresses at the slab mid-span over time

Observing the results of the total stress installed in the slab over time in model 1 (base model) it is clear that, if the shoring system is removed at 28 days (when concrete has already reached its characteristic strength) no cracking is expected to occur in the slab. In fact, during this period, the maximum tensile stress does not exceed 300 kPa, which is a value far below the tensile strength of concrete. However, it turns out that, after the removal of the shoring system, tensile stresses are clearly higher than the value of the axial tensile strength (f_{ctm}). However, it was observed that the tensile stress due to temperature effects represents only 10% of the total stresses, the remaining portion being due to bending moments resulting from loads that act on the slab. Consequently, the actual concrete tensile strength should be a value closer to the flexural tensile strength than to the axial tensile strength. Thus, taking into account the impact of the parcels of flexural and axial tensile, the effective strength of concrete at 28 days is around 3600 kPa, therefore well above the value of f_{ctm} (2600 kPa). Therefore, it is expected that the slab does not crack soon after the total removal of the shoring.

3.2 Parametric study

Based on model 1 (base model), several alternative studies were carried out where the conditions of the problem were changed, namely the slab thickness (model 2), the period of the year when casting occurred (model 3), the spacing between the props (model 4), the date and plan of the total shoring removal (model 5) and the slab boundary conditions (model 6).

Model 2 evaluates the effects on the stress and strain distributions when the slab thickness is changed from 0.20 m to 0.17 m. Figure 9 shows the comparison between the stresses in both top and bottom faces of the slab, in models 1 and 2, in the middle section of the slab for the characteristic combinations of stress resultants. It is noticed that the tensile stresses in model 2 increased on average 20% compared to the ones from model 1. In fact, the maximum tensile stress in model 1 (slab with 20 cm) is 4.1 MPa and in model 2 (slab with 17 cm) 4.8 MPa, when the effective tensile strength of concrete is only 4.0 MPa. So, it turns out that the possibility of the slab cracking is significantly higher when the thickness is reduced, as expected.

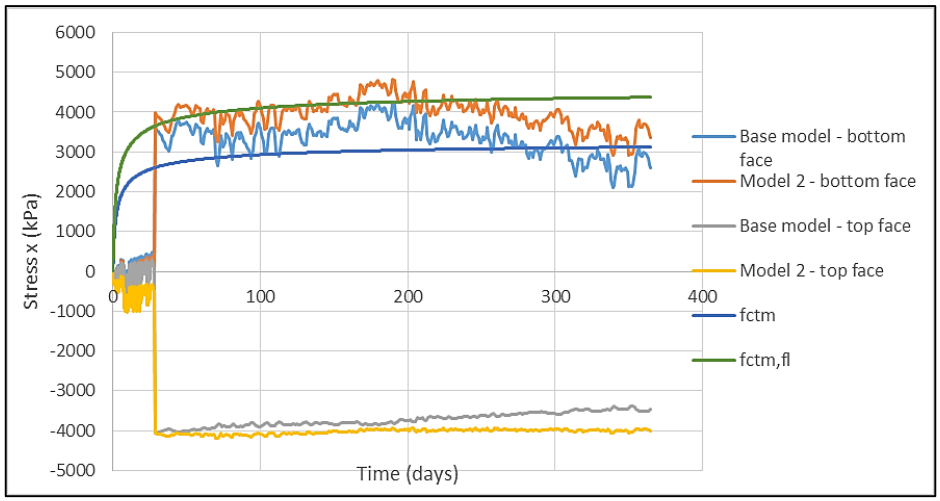

Figure 9 - Comparison of tensile stresses at mid-span of the slab for the rare combination in the base model and model 2

It is expected that a decrease in its thickness will lead to an increase of the deformations of the slab. Figure 10 plots the difference of deformations in the mid-span of the slab, for the base model and for model 2, when compared to the linear elastic model (which does not take into account the evolution of the mechanical properties of concrete and creep). It is noted that the deformations in the base model are approximately 20% lower than in model 2, after total removal of the shoring.

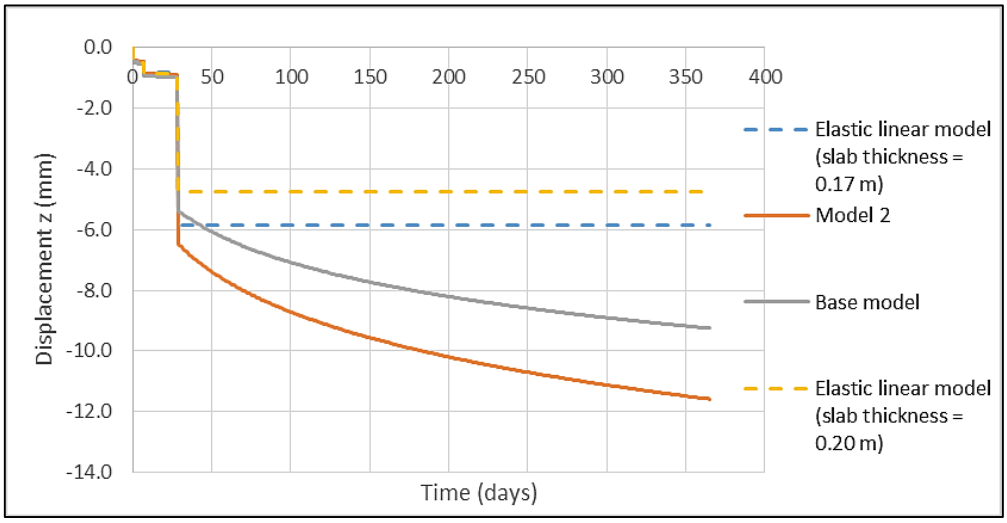

Figure 10 - Deformation at mid-span of the slab for the quasi-permanent combination in the base model and model 2

In the second study variant of the base model, the influence of the thermal stresses when the slab is cast during winter (more specifically in January) is evaluated. The idea is to understand whether the greatest tensile stresses that develop in the winter can be sufficient to cause concrete cracking at the early ages.

Figure 11 represents the total stresses installed at mid-span of the slab, for model 3 and the base model, for the characteristic combination. It is noted that the maximum stresses in the two models are not significantly different, but occur in distinct periods of time. In fact, casting of the slab in winter increases the stresses and the likelihood of cracking at a much earlier stage than when casting occurs in periods of greater heat. This can cause premature cracking of the slab and an increase of long term deformations.

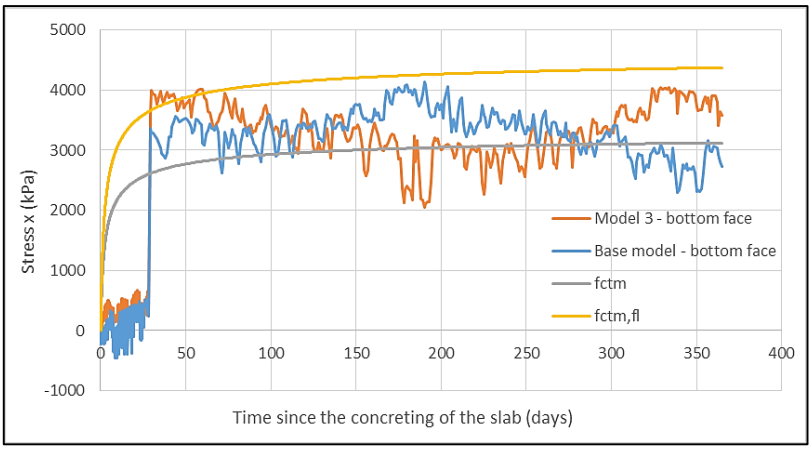

Figure 11 - Comparison of tensile stresses at mid-span of the slab for the rare combination in the base model and model 3

In the models previously studied 1.5 m spacing between the props was considered. The next model intends to study the impact of the spacing of the props on the stress and strain distributions in the slab. To that effect, two studies were carried out: in the first case, the props are spaced of 1.0 m until their withdrawal at 7 days (model 4.1) and, in the second case, the spacing is modified to 2.0 m (model 4.2)

Figure 12 shows the stresses at the bottom face at mid-span of the slab for the rare combination for model 4.1 and the base model. The differences between the two models are very small even before total shoring removal. Despite this, there is a slight decrease of stresses in model 4.1 compared to the base model due to the reduction of the residual stresses installed in the slab, before the total withdrawal of the shoring system. However, this decrease is very small and therefore it can be concluded that the increase of props compared to the base model, does not bring any significant improvement in terms of stress resultants and deformations reduction. This conclusion strengths the need for a correct design of the number of props to avoid unnecessary coasts.

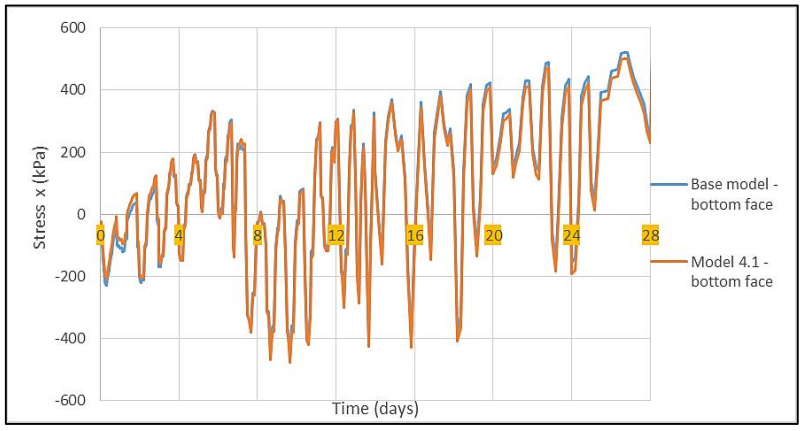

Figure 12 - Comparison of tensile stresses at mid-span of the slab for the rare combination in the base model and model 4.1

Figure 13 represents the tensile stress at mid-span of the slab for the rare combination for model 4.2 and the base model. These results show that there is an increase of the stresses in model 4.2 before the complete withdrawal of shoring. In fact, during this period the maximum stresses in model 4.2 were about 0.79 MPa and in the base model 0.45 MPa, and, on average, the tensile stresses in model 4.2 were about 30% higher when

compared to the base model, until 28 days. Nevertheless, it appears that the stresses in the two models are not very distinct and tend to the same values over time. However, the decrease of the props increases the residual stresses, the deformations and the risk of premature cracking, mainly at the early ages. So, this factor should be taken into account in the design of the shoring system.

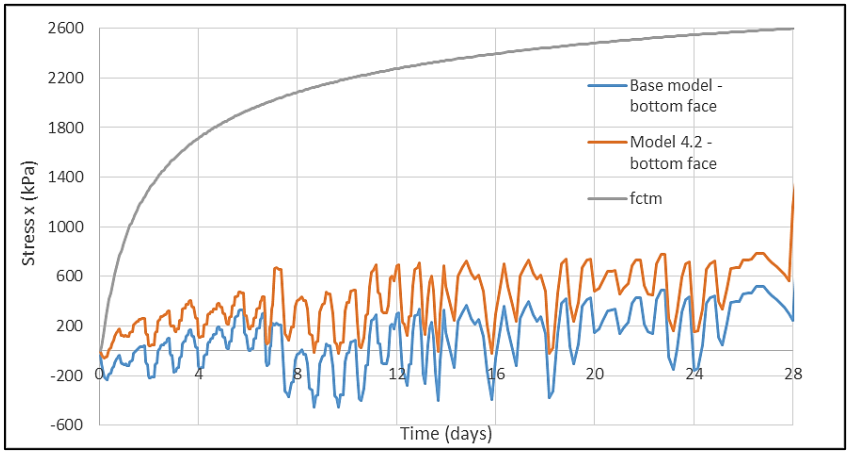

Figure 13 - Comparison of tensile stresses at mid-span of the slab for the rare combination in the base model and model 4.2

In the fifth parametric study, the influence of the date and sequence of shoring removal was analysed. Four alternative removal schemes were considered. Table 6 lists the date of withdrawal of props in models 5.1, 5.2 and 5.3. The partial removal of the shores corresponds to withdrawing approximately 60% of props and the formwork is always removed at the same date in which the shores are completely removed.

Table 6 - Withdrawal scheme of the shores

	Model 5.1		**Model 5.2**		**Model 5.3**	
	Partial removal	Complete removal	Partial removal	Complete removal	Partial removal	Complete removal
Time (days)	14	21	7	14	3	7

Concerning model 5.4, two alternative scenarios of shoring removal sequence were studied:

- Model 5.4.1: shores are progressively removed from 14 to 16 days and the sequence of removal is from the lateral to the central shores;
- Model 5.4.1: shores are progressively removed from 14 to 16 days and the sequence of removal is from the central to the lateral shores;

Figure 14 shows the tensile stresses installed in the slab for models 5.1, 5.2 and 5.3. It is found that, by removing the shores before 28 days, the likelihood of slab cracking in that period increases significantly when compared to the base model. Thus, while the base model had a maximum stress of 300 kPa up to 28 days, in models 5.1-5.3 the maximum stress is above 3000 kPa, clearly above the axial strength of the concrete (f_{ctm}). In model 5.3 stresses are even higher than the flexural strength of concrete ($f_{ctm,fl}$) and so the chances of premature cracking are very significant, in a period of time when concrete's full characteristic strength has not been reached. Thus, in this situation, the slab may crack before 28 days, so the design of the slab should not be made without considering the total history of stresses.

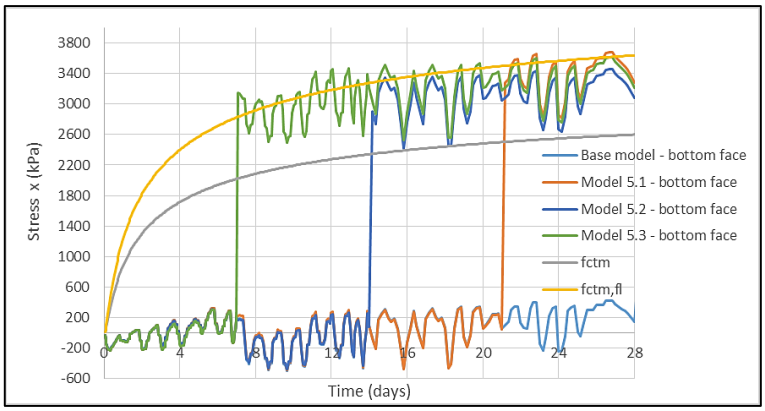

Figure 14 - Comparison of tensile stresses at mid-span of the slab for the rare combination in the base model and models 5.1-5.3

Figure 15 shows the deformations over time at mid-span of the slab for the base model and for models 5.1-5.3. There is an increase of long-term deformations when the shores are removed earlier. However, the values in Figure 15 do not take into account possible cracking and the consequent increase of deformation due to the reduction of the structure's stiffness. In fact, especially in model 5.3, premature cracking in the slab would be expected to occur, which would increase significantly the long-term deformations in comparison to the values shown in Figure 15.

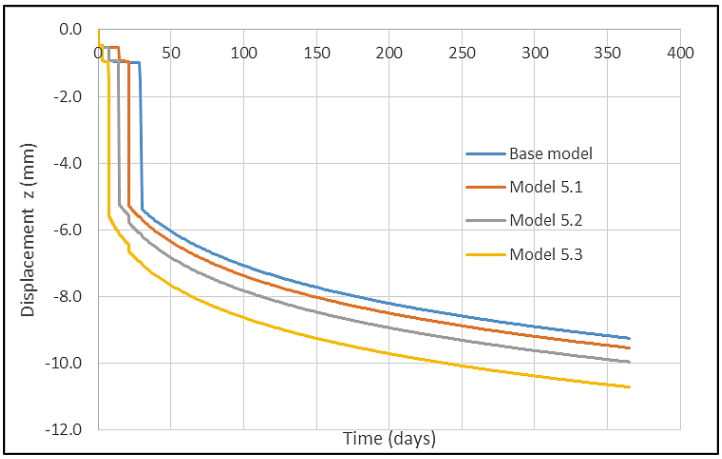

Figure 15 - Deformation at mid-span of the slab for the quasi-permanent combination in the model 1 and models 5.1-5.3

In what concerns model 5.4, considerable differences in the behaviour of the slab when the shores are removed from the edge of the slab to the centre can be observed. In fact, when the shores are removed from the edge to the centre, the slab works in a reverse way to the one it was initially designed for. In this situation, the props act as columns and therefore unpredicted negative bending moments can appear in the central section of the slab. Another essential aspect related to the sequence of removal of the shores is that, when the shores are removed from the edge to the centre, the load is essentially unloaded on the central shores and these shores will consequently be subjected to a considerable increase of axial forces. This can lead to serious stability problems of these structural elements. Observing the vertical reactions in the central props of the slab, it can be seen that in model 5.4.1 (removal edge-centre) the props have an axial force of 15.0 kN, immediately before total removal of the shores. However, at the same time, the shores in model 5.4.2 (removal centre-edge) have an axial force of 31.0 kN, i.e., two times higher. Taking into the maximum strength of the shores, it

turns out that the metal shores considered in this parametric study resists at most an axial force of approximately 18.5 kN. Therefore, in model 5.4.2, the central shores have a great probability of exhibiting stability problems.

Therefore, it is concluded that the removal of the shoring system must be carried out in a way that does not cause large increases in the axial loads or modify the static behaviour of the slab. To that effect, the shoring of the slab must be removed from the point where the curvature is greater to the regions where it is smaller.

Finally, model 6 assesses the consequences of changing the boundary conditions of the slab. It is assumed that the slab is end-fixed on all edges. In this way, the greater stresses and bending moments occur on the edge of the slab, so cracking is expected to appear in regions near those supports.

Figure 16 represents the stresses (in the upper and lower face) at mid-span and on the external boundary of the slab for the quasi-permanent combination. Comparing the results from Figure 16 to the ones of the base model, it is clear that there is a very considerable decrease of slab tensile stresses in the central zone. In fact, the stresses in the mid-span of the slab in model 6 are, on average, 35% lower than the stresses in the base model, right after the removal of the whole shoring system.

Although there is a significantly decrease in the tensile stress at mid-span of the slab in model 6, the opposite occurs in the area next to the slab boundary that suffers a very considerable increase of the tensile stress in comparison to the base model. Comparing the maximum stresses in both models, soon after total withdrawal of the shores, model 6 has a maximum stress of 2400 kPa (near the support) while the base model has a maximum value of 2880 kPa (1.2 times greater). Thus, despite the fact that there is an increase in tensile stresses in the slab border, by analysing the entire slab it is noted that in model 6 the maximum stresses are lower than the ones obtained with the base model. So, it is expected that in the case of cracking, the width of cracks in model 6 is smaller than in the base model. Table 7 shows the maximum expectable cracks width in the slab with model 6. Observing the results presented in Table 7, it turns out that the maximum crack width is 0.19 mm in model 6. The base model has a crack width of 0.24 mm, i.e. 0.5 mm greater than in model 6. However, the crack width limit is 0.4 mm (EN 1992-1-1), so in both cases the crack width is admissible.

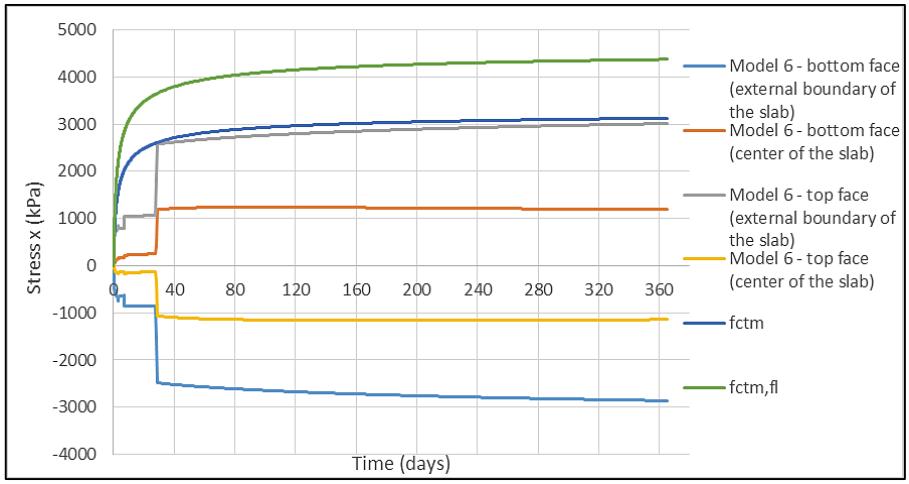

Figure 16 - Stresses in quasi-permanent combination for model 6 at mid-span and at the border of the slab

Table 7 - Verification of crack width limit for the quasi-permanent combination

ϕ (mm)	s (m)	σ_s (kPa)	k_t	k_1	k_2	$s_{r,max}$ (m)	w_k (mm)
12	0.2	204867.0	0.4	0.8	0.5	0.314	**0.19**

4. Conclusions

In conclusion, it was observed that if the whole shoring system is removed only after 28 days (when concrete has already reached its characteristic strength) and the props are appropriately designed it is unlikely that any cracks occur in the slab until complete removal of the shores. Therefore, if the shoring is only fully removed at 28 days, the design analysis of the slab can be performed without consideration of the whole history of stresses installed on the slab until the 28 days, as usually happens in current building structures design.

However, if the shoring system is removed at early ages, it is necessary to perform a prior study of the maximum stresses installed in the slab during the constructive stage, before complete withdrawal of the shoring system due to the high probability of premature cracking of the slab. This possible cracking of the slab, before 28 days, is not usually considered in the current structural design procedures, which can lead to incorrect results essentially in the verification of the serviceability limit states.

The results confirmed that the common practice of shoring (which consider total shoring removal only after concrete has reached its characteristic strength) corresponds in fact to the best practices as it reduces the stresses and residual strains and avoids cracking in the slab before the 28 days. Any other practice, leading to an early withdrawal of the shoring, shall be preceded by a preliminary study of the strength and the stresses installed on the slab at the moment of the shoring removal.

References

ADINA. (2011). *Theory and Modelling Guide.* USA: ADINA R&D, Inc.

Azenha, M. (2009). *Numerical simulation of the structural behaviour of concrete since its early ages.* PhD in Civil Engineering, FEUP, Porto.

Bazant, Z., & Chern, J. (1985). Log double power law for concrete creep. *ACI Journal*, 82-59.

De Schutter, G., & Kovler, K. (2001). *Short term mechanical properties. Early age cracking in cementitious systems.* A. Bentur, RILEM Publications.

EN 1992-1-1 . (2004). *Eurocode 2 - Design of concrete structures - Part 1-1: General rules and rules for buildings.* Comite Européen de Normalisation (CEN).

Honorio, T., Bary, B., & Benboudjema, F. (2014). Evaluation of the contribution of boundary and initial conditions in the chemo - thermal analysis of a massive concrete structure. *Engineering Structures 80*, 173-188.